Field Evaluation of Thermal Deformations in Undoweled PCC Pavement Slabs

M. Poblete, R. Salsilli, R. Valenzuela, A. Bull, and P. Spratz

This paper presents some of the results obtained in extensive research of the Chilean in-service network of PCC paved roads, in which measurements have been conducted in 21 test sections covering various conditions of climate, pavement structure, and age. In test slabs, simultaneous measurements were made of internal temperatures and absolute vertical displacements of slabs, as well as openings of transverse joints and faultings. The results show a "permanent" upward curling of slabs in all pavements sections included in the study, as modified by daily temperature variations. The curling is demonstrated in the field by the perceptible rocking of the slabs under the early morning traffic and by the systematic transverse cracking and corner breaks of some rather new pavements with no signs of pumping. Cracking seems to start from the surface downward and from the edges inward. Detailed evaluation of the internal stresses with the superimposed nonlinear effects of environmental and wheel loads, calibrated with these results, is under way.

About one-third of Chile's 6,700-km network of paved roads are Portland cement concrete, located mainly in the central and southern regions and carrying the heaviest traffic, especially along the Pan-American Highway.

Toward the end of the 1970s, an extensive reconstruction program of the most deteriorated sections of the network was started by the Highway Division of the Chilean Ministry of Public Works, and it is now almost complete. In order to define maintenance policies for these sections, a Maintenance Management System is being implemented (*1*). To this end, the Highway Division assigned the Universidad de Chile to model the structural deterioration of concrete pavements, which had been designed and constructed under general AASHTO guides and specifications. Therefore, monitoring the pavement for the effects of climate, traffic, and subgrade support was considered (*2*). Development and calibration of the predictive analytical model required implementation of survey and measurement methodologies which are now performed periodically at 21 locations along the concrete pavement network. In addition, these local surveys and measurements are expected to facilitate the calibration of mechanized equipment, such as a Lacroix-type deflectometer and a profilometer, which are used extensively by the Highway Division.

Ambient temperatures in the concrete paved roads are mild, with no big differences along the instrumented sections, and are free of frost conditions affecting the soil. Figure 1 shows the number of days with heavy rains (>5 mm/24 hr) increasing southward (*3*), from an average of less than 15 days in test section 1 to more than 120 in test section 21, mostly during the winter. Consequently, ambient humidity is far from saturation during the rest of the year, with strong hydro-evaporation conditions predominating.

After 3 years of periodic monitoring, local surveys and measurements have shown that an upward curling of the slabs prevails during most of the daily thermal cycle; part of this deformation is permanent, but the remainder varies daily in accordance with changes in the thermal condition. Identical effects have been reported from California by Hveem (*4*), Tremper and Spellman (*5*), and others. This condition of partial support exhibited by deformed slabs accelerates concrete fatigue, thus reducing the number of theoretically allowed loading cycles. Cracking occurring before the third year of service in some pavements subjected to heavy traffic could be explained by these findings.

In order to consider these effects in predictive deterioration models, calculations are in progress to evaluate internal stresses through finite-element techniques, fitting the measured deformations with those computed under equivalent conditions of edge restraints, support, and loading. This work constitutes the follow-up step of the research program and will be the subject of future research.

FIELD MEASUREMENTS AND RESULTS

Along the heavily trafficked central-south regions of Chile (shown in Figure 1), 21 test sections (TS) were selected to be monitored for the effects of weather conditions, pavement aging, and slab support stiffnesses. In Table 1, location and pavement structural characteristics for the 21 test sections are shown. The instrumentation designed and installed in each of the 21 test sections (*6*) allows the measurement of internal temperatures and absolute vertical displacements of slabs, as well as openings of transverse joints and faultings, using the elements shown in Figure 2. For deep reference bases (DRB), drilling was performed using percussion-rotation and compressed air, to cause the least alteration to subgrade soils; likewise, borehole reconstruction was performed to reproduce pavement conditions as closely as possible.

The diagram shown in Figure 3 illustrates the analog-digital data acquisition system used for the simultaneous measurement of temperatures, thermal displacements, and load deflections; values are processed in-situ by a portable PC. Signal monitoring allows qualification of the results, recording of results for further analysis, or repeating of measurements.

M. Poblete, R. Salsilli, and R. Valenzuela, Instituto de Investigaciones y Ensayes de Materiales (IDIEM), Universidad de Chile, Casilla 1420, Santiago, Chile. A. Bull and P. Spratz, Direccion de Vialidad, Ministerio de Obras Publicas, Casilla 72, Santiago, Chile

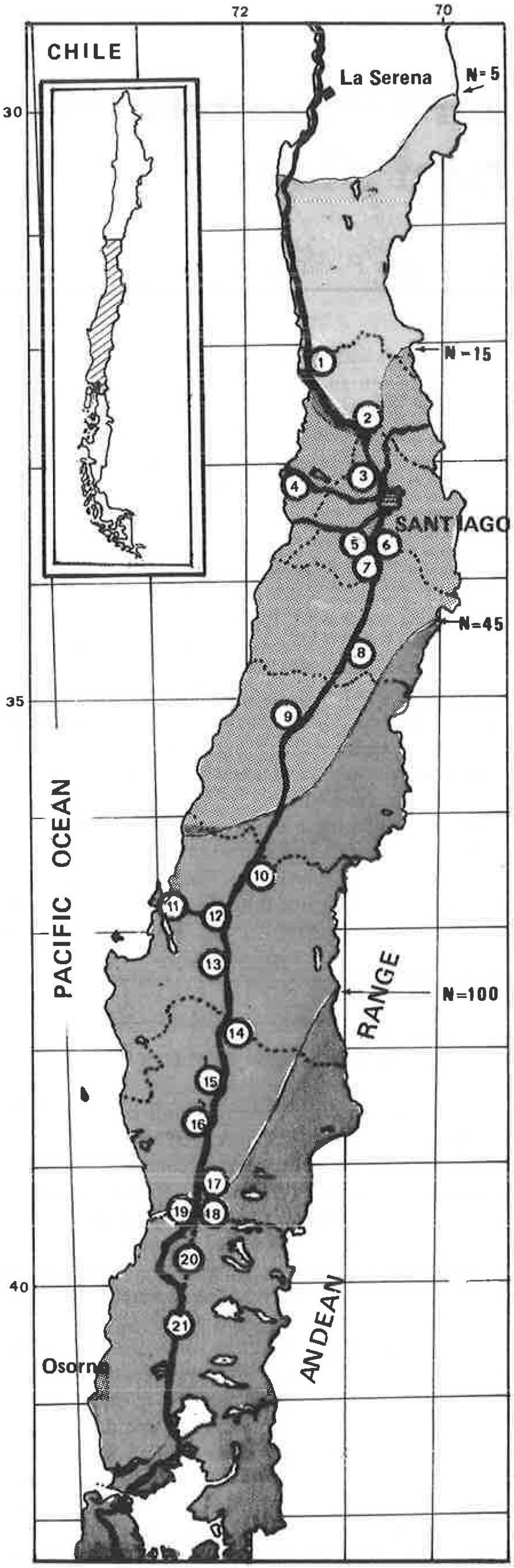

FIGURE 1 Map of test sections and days per year (N) of heavy rainfall.

Once a measurement cycle has been completed, instruments, cables, and connectors are taken to the next test section, leaving only the reference bases in place with the LVDT housings enclosed by lids mounted flush with the pavement.

The data presented herein were gathered during summer 1986, winter 1986, and summer 1987, over a continuous 24-hr cycle. Accuracy of the measurements by their frequency is shown in Table 2.

Typical internal slab temperatures, recorded during 24 hr on a sunny summer day, are plotted in Figure 4 by depth of measurement. Minimum mean temperature occurs early in the morning, whereas maximum mean temperature occurs typically between 3 p.m. and 5 p.m. The temperature range on the slab surface becomes 4 times higher than the temperature range at the slab bottom, and the temperature distribution never becomes linear with depth or constant in slab thickness.

Therefore, thermal gradients exist within the slab during the 24-hr period. Negative gradients—when the slab surface is cooler than the bottom—tend to predominate from late afternoon to late morning through the night (Fig. 4) and during the whole year. Accumulated hours at various thermal gradients are presented in Figure 5; the histogram is the result of semiempirical modeling calibrated through actual field measurements (*7*). Positive gradients, though higher in absolute value, exist for only a few hours on a sunny summer day.

As a consequence of daily variations in thermal gradients, pavement slabs undergo continuous deformations, as may be derived from the isograms in Figure 6, which were obtained on a summer day in 1985 by precise measurements (to ±0.01 mm) of nine topographical reference bases installed in a slab. These isograms show the upward concave shape of the slab for the early morning negative gradient (Figure 7a), and a nearly cylindrical shape of longitudinal axis during the afternoon hours with positive gradient and high mean temperature, when the rotation of the slab's transverse edges is prevented by the locked joints (Figure 7c). Such behavior is typical and was observed in all instances of high mean temperatures. Rotation is not prevented at the longitudinal joint where two slabs belonging to adjacent lanes and paved at different dates are linked together through steel tie bars.

Horizontal slab movements measured at transverse joints near the slab outer edge are shown in Figure 8, for five moments of a complete cycle during a sunny summer day. Sections remain plane at all times, but rotate with the gradient. With negative gradients the joint can be completely open if the mean temperature is low enough, whereas the bottom edges can be compressed if the mean temperature is high. For positive gradients and high enough mean temperatures, the joint can close, thus preventing any rotation (locked joints).

On cloudy winter days the temperatures are low and very stable, as are the gradients, and hence the edges do not rotate significantly. However, the joints stay open and there is little or no compression at the lower edges. Note that the absolute value of joint openings at given temperatures is not equal for all pavements, but depends on conditions such as the level of maximum temperature in the fresh concrete, drying shrinkage (*5*), or swelling due to seasonal moisture absorption (*8*).

Figure 9 illustrates joint opening variation in the mean plane, divided by the mean length of the slabs adjacent to the instrumented joint. A linear relationship with the mean temperature for winter and summer was obtained. On sunny summer

TABLE 1 LOCATION AND STRUCTURAL CHARACTERISTICS OF TEST SECTIONS

Number	Geogr. Coordinates		Slab construction	Pavement				Infrastructure		
01	32° 22'	71° 21'	Spr'83	0.23	3.7 - 4.6	Y	CTB	AC*	ML	---
02	32° 52'	70° 49'	Spr'81	0.23	4.5 - 5.4	N	CTB	PCC*	CL	---
03	33° 13'	70° 44'	Win'84	0.24	3.4 - 3.6	Y	CSB	PCC	CH	3.4
04	33° 15'	71° 23'	Sum'85	0.26	3.4 - 3.6	Y	CSB	GRM	SM	3.0
05	33° 40'	70° 55'	Spr'75	0.22	3.4 - 5.4	N	GRB	GRM	GC	---
06	33° 48'	70° 45'	Aut'83	0.24	4.2 - 4.6	N	GRB	AC	SP	---
07	34° 04'	70° 42'	Aut'83	0.25	3.6 - 4.6	N	GRB	PCC	GP	---
08	34° 34'	70° 58'	Sum'83	0.23	3.7 - 4.3	N	CTB	PCC	SM	---
09	35° 21'	71° 31'	Aut'83	0.23	3.7 - 4.6	Y	CTB	AC	SM	---
10	36° 32'	72° 04'	Aut'82	0.21	4.5 - 4.6	N	GRB	PCC	GP	2.0
11	36° 49'	73° 01'	Spr'84	0.23	3.5	Y	CTB	AC	ML	---
12	37° 02'	72° 26'	Aut'84	0.22	3.5 - 3.6	Y	CSB	PCC	SC	2.6
13	37° 10'	72° 24'	Win'82	0.21	4.4 - 4.6	N	CTB	PCC	SP	2.5
14	37° 50'	72° 02'	Aut'79	0.21	4.3 - 4.8	N	CTB	PCC	SM	---
15	38° 14'	72° 22'	Aut'84	0.23	4.0	Y	CSB	PCC	ML	---
16	38° 46'	72° 34'	Aut'81	0.21	4.4 - 4.6	N	CTB	PCC	CL	---
17	39° 07'	72° 41'	Aut'83	0.22	4.5	Y	GRB	GRM	GM	3.0
18	39° 22'	72° 38'	Spr'84	0.22	3.8 - 4.3	Y	CTB	GRM	CL	---
19	39° 33'	72° 56'	Aut'83	0.23	4.4 - 5.0	N	CTB	PCC	ML	---
20	39° 40'	72° 56'	Spr'83	0.23	4.3 - 4.6	N	GRB	GRM	GM	2.0
21	40° 02'	72° 58'	Sum'83	0.22	4.5	N	CTB	PCC	ML	1.5
Test Section	Latitude South	Longitude West	Season 'Year	Thick- ness (m)	Joint Spacing (m)	Edge Drain	Base	Sub Base	Sub Grade (USCS)	Water T. Depth (m)

*Old "AC" or "PCC" pavements overlayed with "PCC".

days, when slab temperature increases sufficiently and the lower edges of the slabs come into contact, compression builds up, and the openings decrease nonlinearly until the joints are completely locked. The experimental straight lines obtained for a given test section with mean temperatures below the locking temperature have equal slopes of

$$\alpha = 1.14 \times 10^{-5} \, (^{\circ}\mathrm{C})^{-1}$$

This value is very close to the thermal expansion coefficient of concrete, determined in the laboratory under free-expansion conditions, and is among the largest values reported in the literature (*9*) for siliceous high-hardness aggregates, which are predominant in Chile. Hence, the eventual restrictions of slab expansion in the field, due to friction between the base and the contact area whose magnitude depends on the degree of upward curling, appear to be of minor significance in this case. When comparing the data obtained at different dates and therefore under different pavement moisture conditions, the vertical distance between the winter line and the summer line, considered as a dry reference state, would represent the swelling of concrete. This behavior was observed in all 21 test sections (*10*).

The vertical movements of two typical pavement slabs, obtained from points DRB 2, 3, 4, and 5, are shown in the upper part of each graph illustrated in Figures 10 and 11, with ordinates that are increasing upward and refer to the smallest value for the corresponding day. The curves represented in the lower part of each graph, with ordinates that are increasing downward, correspond to the maximum deflection under the slow-moving load of an 81-kN axle, measured at the same four points of the slab. To better assess the evolution of thermal conditions throughout the day, the gradient and the mean temperature have been superimposed in graphs DRB 4 and DRB 5, respectively. This allows observation of the following details:

- Vertical movements of slab corners and edges (DRB points 2, 5, and 3) oscillating all day following thermal gradient variation become minimal when this gradient becomes maximum or positive. When the gradient is negative, the corners and edges stay uplifted and the slab then presents a perceptible upward curling that matches the previous results obtained from topographical levelings.
- The slab remains curled upward when the thermal gradient becomes null, as was observed at 10 a.m. (warming) of the summer day cycle (Figure 10).
- Behavior of the central point, DRB 4, is always contrary to the behavior of the corners and the edges. Therefore, when

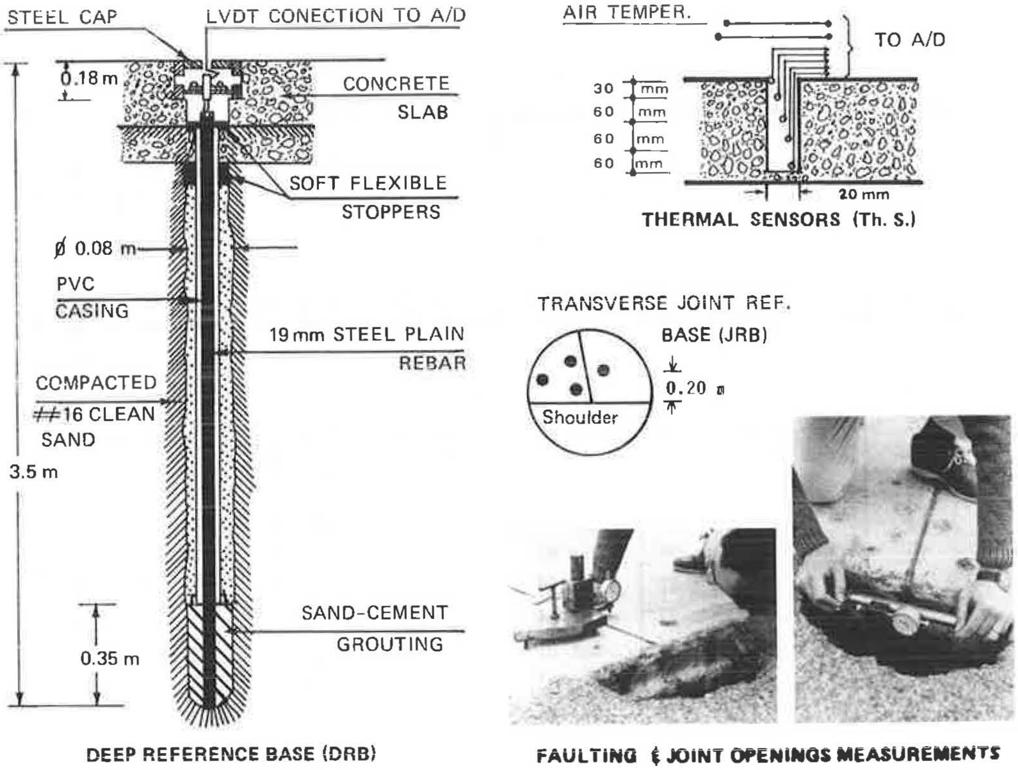

DEEP REFERENCE BASE (DRB)

THERMAL SENSORS (Th. S.)

FAULTING & JOINT OPENINGS MEASUREMENTS

FIGURE 2 Instrumentation devices in the test sections.

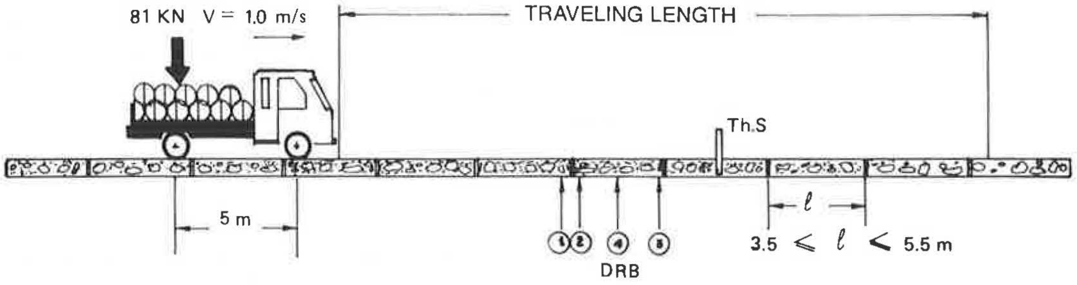

LAY OUT OF INSTRUMENTATION AT EACH TEST SECTION

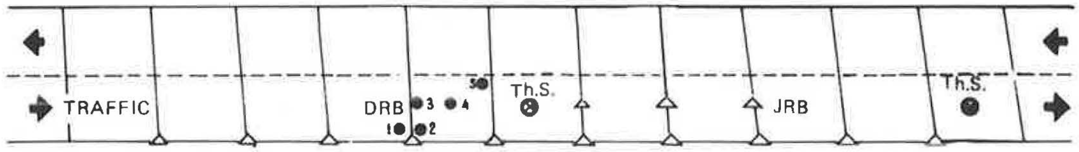

TRB: Topographical Reference Bases

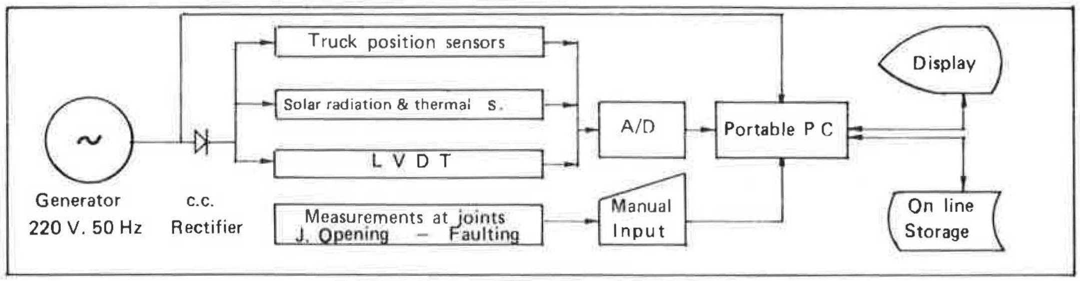

FLOWCHART OF THE DATA ACQUISITION SYSTEM

FIGURE 3 Schematic layout of instrumentation used.

TABLE 2 LIST OF MEASUREMENTS CARRIED OUT IN ALL TEST SECTIONS

Measure	Accuracy	Frecuency
Temperatures	± 0.20 °C	every 5 min
Displacements	± 0.01 mm	every 5 min
Deflections	± 0.01 mm	every 1 hour
J. Openings	± 0.05 mm	every 2 hour
Faultings	± 0.10 mm	once a day

corners and edges are supported, due to some strong positive gradient, the slab center rises; so does DRB point 3 in some cases, causing the nearly cylindrical shape illustrated in Figure 7c.

- Maximum deflections under load, determined at DRB points 2, 5, and 3, show a behavior that is very similar to that due to thermal gradient, and there is a proportionality between the magnitudes of deflection and edge lifting.
- Deflections in winter may not at any time during the day reach such low values as may be derived from Figure 11. This would indicate that the condition of partial support at the center of the slab may last the whole day, as it occurred in the case presented here.

The deformation at the corner point DRB 1 of the adjoining slab is similar to the behavior at point DRB 2, though generally of different magnitude, as it appears from Table 3, which summarizes all data obtained for the 21 test sections. To analyze this apparent anomaly in homogeneous pavement sections, deformations were normalized by using a standard orthogonal 3.50-m × 4.50-m slab as a reference. In Figure 12, all pairs of points DRB 1 to DRB 2 of normalized maximum deformations are plotted against each other. Having eliminated the geometric difference for every deformation, the discrepancy that still persists has to be explained by the interlock created in the joint crack with some preferential inclination to one side.

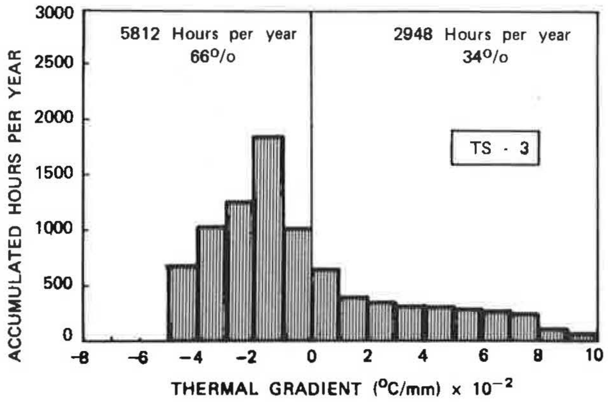

FIGURE 5 Histogram of modeled thermal gradients for typical test sections.

A different behavior is observed at the opposite corner in the same slab. Figure 13 shows the marked symmetry that exists in the upliftings of points DRB 2 and 5 in opposite corners, thus illustrating the reduced restriction imposed by the tie bars built in the longitudinal construction joints between two-lane pavements. In the special case of four-lane dual-carriage ways represented by test sections 2 and 11, some rocking of the instrumented outer lane would be produced by the central lane during intense cooling after a hot summer day.

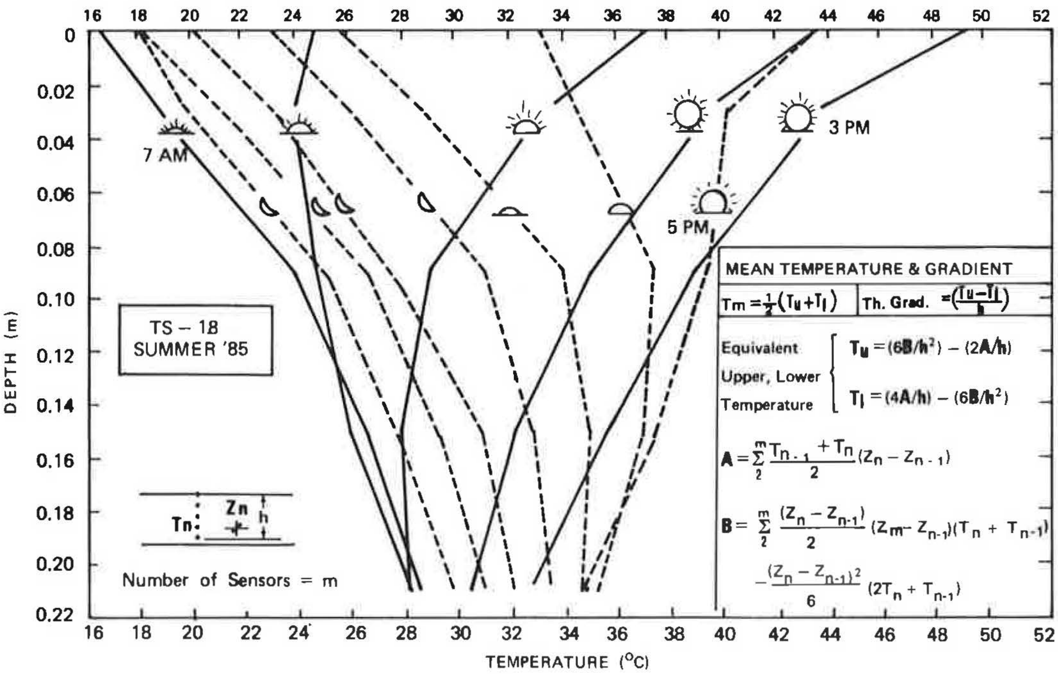

FIGURE 4 Internal temperature distribution every 2 hr during a measurement cycle.

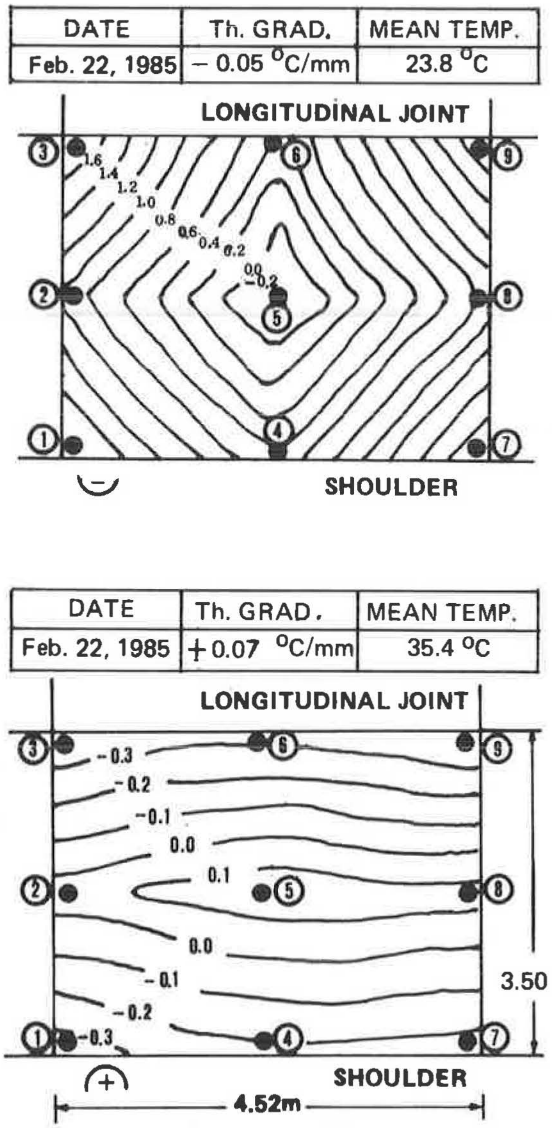

FIGURE 6 Isograms of a typical slab deformed by temperature (°C/mm).

FIGURE 7 Typical shapes of slabs deformed by temperature.

From Table 3 it can also be seen that the upward-curling deformation occurs with greater or less significance in all pavements, and it occurs in the south at magnitudes similar to those in the north, in spite of climatic differences. Furthermore, the duration of this phenomenon covers the main part of the day, at least 14 hr in summer and the whole day during winter.

Figures 14, 15, and 16 show the relationships between slab deformation and thermal gradients for different geographical locations, as well as relationships with pavement age and base types. The behavior of the corners and of the whole transverse edge during the morning warming is different than the behavior during the evening cooling. This is due to the lower rotation restriction existing at joints when they stay more open (low mean temperature in the early morning). As surface temperature increases, the slab edges go down, and the joints get compressed and tend to lock up. In the afternoon, surface cooling reverses the process, but in a different way because the thermal inertia of concrete causes a very slow decompression in the slabs. In this case, the upward curling remains restricted while the gradient is decreasing. This phenomenon occurs in the three cases with respect to summer and is representative of all 21 test sections (*10*). In winter, owing to low mean temperatures, the open joints do not restrict the deformation; therefore both branches tend to coincide on a single straight line.

Furthermore, from Figures 14 and 15, it may be seen that the slabs require a certain positive gradient in order to reach the condition of full support. This would prove the existence of a thermal-independent cause of upward curling. Its origin could be the moisture differential through the slab thickness, since the upper portion is nearly always drier than the bottom. On the other hand, excessively high fresh concrete temperatures that are frequent on hot summer days undoubtedly contribute to a larger shrinkage and to more open joints. Consequently there is less restriction on the slabs' transverse edges and greater freedom to rotate and to uplift, regardless of the thermal gradients. Similar effects are clearly experienced early each autumn when the pavement reaches its maximum dryness.

This upward curling was also found in an older pavement, but as shown in Figure 16, it is almost negligible when compared to the other ones. The difference is assumed to be related in some way to the modern use of membrane-forming curing compounds under prevailing environmental conditions of high evaporation, as compared with the old practice of polyethylene film coverings or dikes for pond curing wherein temperature can be regulated (*9*).

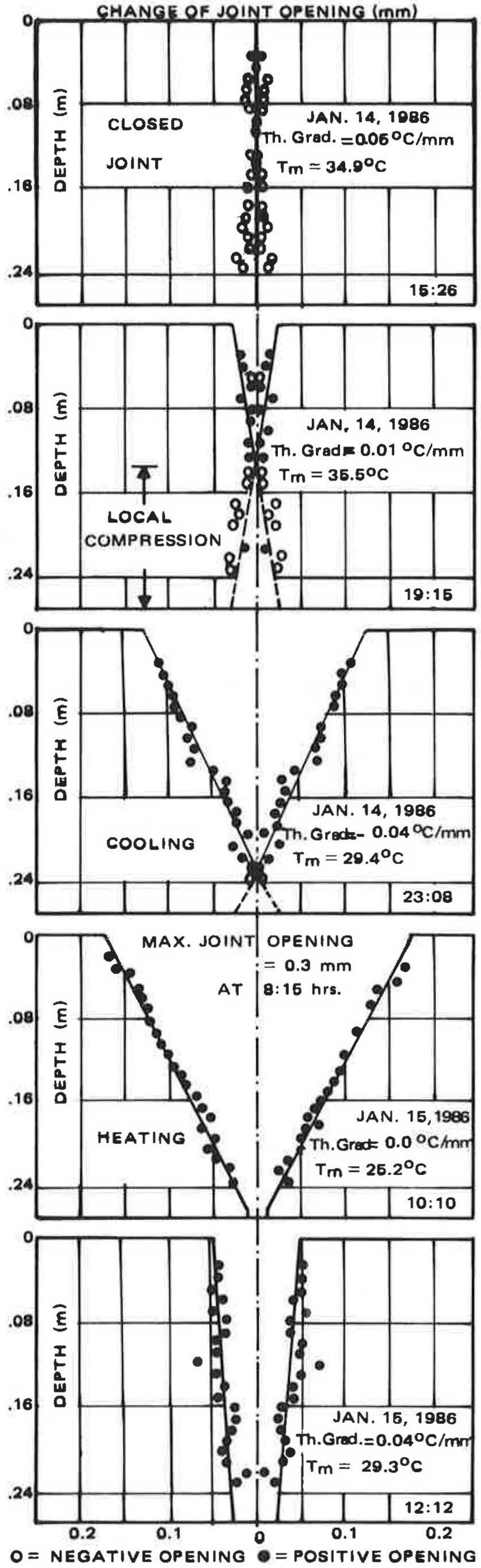

FIGURE 8 **Movement pattern of a joint during a 24-hr cycle, measured by outer edge.**

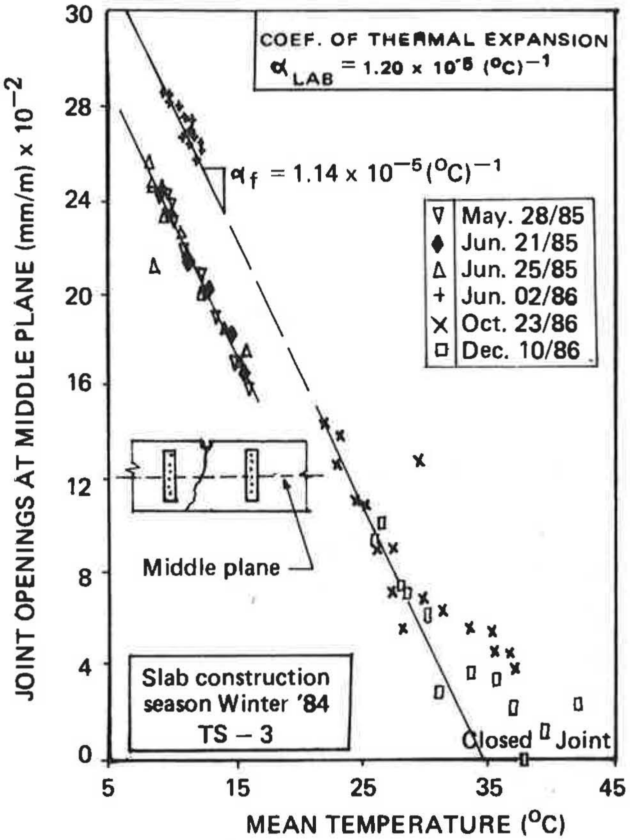

FIGURE 9 **Longitudinal thermal deformation of a typical PCC pavement measured at joints.**

CONCLUSIONS

The instrumentation as well as the measurement methodology presented herein have proven to be efficient for quantifying, with a high degree of accuracy and repeatability, the absolute movements and deformations that can occur in concrete pavement slabs.

In all the pavement sections included in this study, the generalized prevailing upward curling of the slabs, causing considerable lack of support at slab edges, has been verified. This condition is reversed only during the hours of high solar radiation.

In order to obtain the effective support of slab edges, a significant positive thermal gradient has to be generated in the concrete slab to overcome a "permanent" upward curling that occurs independently of the thermal one.

Under conditions where positive gradients are higher than the "support initiation gradient," the slabs normally are expanded and rotation at their transverse edges is restricted (Figure 7c); thus a cylindrical shape is imposed on the slab with its longitudinal edges supported. The traditional downward curling may appear only if the transverse edges are free to rotate (Figure 7b), something that seldom occurs when the mean temperatures in the pavement remain low enough during a sunny day.

In view of the foregoing, upward curling with partial support localized in the central zone of the slab, and minimum collaboration of contiguous slabs owing to a relatively more

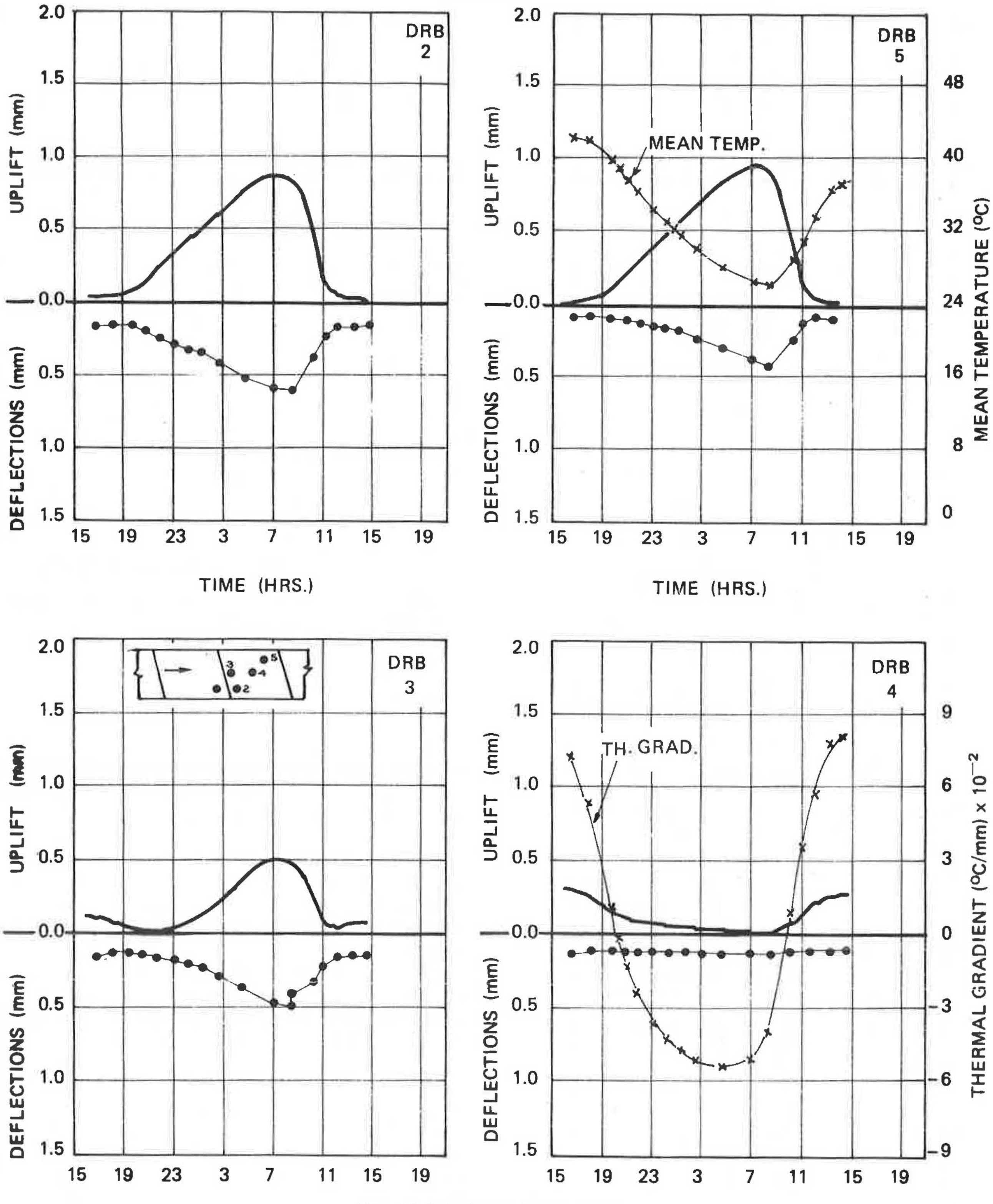

SUNNY

TS–03 SUMMER (DEC, 1986)

FIGURE 10 Continuous slab displacements and load deflections during a summer day cycle, for an 81-kN moving load.

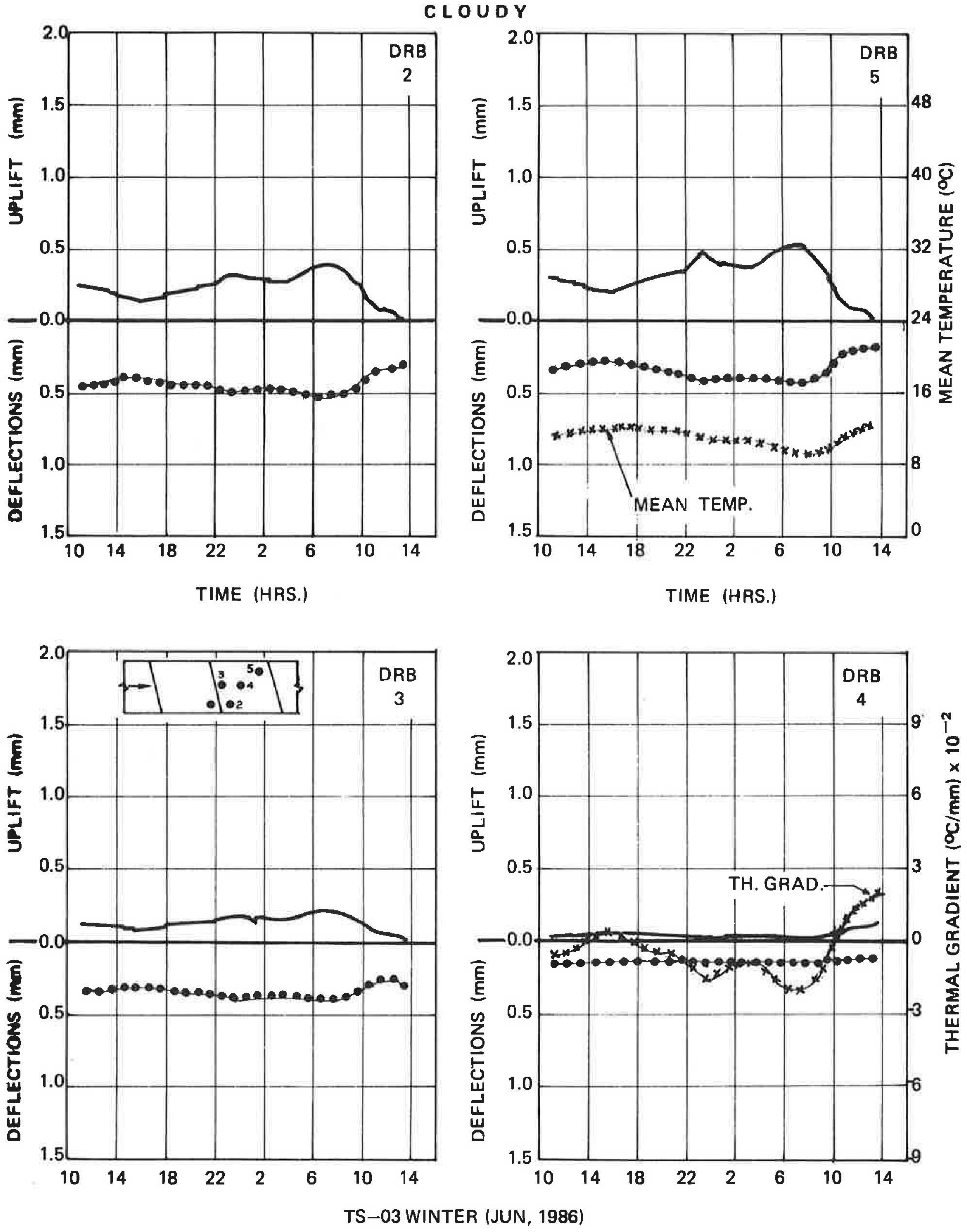

FIGURE 11 Continuous slab displacements and load deflections during a winter day cycle, for an 81-kN moving load.

TABLE 3 MAXIMUM UPLIFT OF CORNERS

Test Section		Slab Length (m)		Slab Construc. Season	Measure Season	Thermal Cond.		Max. Uplift of Corners* (mm)			Accumulated hours
						Mean T.	Grad.				
		L_1	L_2			°C	°C/mm	DRB 1	DRB 2	DRB 5	
Longotoma	1	4.56	4.06	Spr.'83	Sum.'86	22.5	−0.03	1.98	1.13	1.00	21
					Aut.'86	11.5	−0.02	0.95	0.60	0.57	18
					Sum.'87	24.5	−0.03	1.55	0.91	0.90	19
Las Chilcas	2	4.54	5.15	Spr.'81	Win.'86	12.0	−0.04	0.73	0.63	0.82	24
					Sum.'87	28.5	−0.05	0.90	0.88	1.70	16
Lampa	3	3.50	3.49	Win.'84	Aut.'86	9.0	−0.02	0.70	0.42	0.52	24
					Sum.'87	26.5	−0.05	1.05	0.92	0.95	15
Lo Vásquez	4	3.44	3.53	Sum.'85	Sum.'86	23.0	−0.05	1.65	1.30	1.42	19
					Win.'86	6.5	−0.03	0.60	0.45	0.50	24
					Sum.'87	23.7	−0.05	1.25	1.05	1.20	16
Talagante	5	5.00	4.55	Win.'75	Aut.'86	12.0	0.00	0.15	0.45	0.25	24
					Sum.'86	25.5	−0.06	0.64	0.70	0.65	10.5
Paine	6	4.64	4.57	Aut.'83	Aut.'86	7.0	−0.03	0.59	0.52	0.30	24
					Sum.'86	25.5	−0.04	0.63	0.65	0.57	14
Graneros	7	4.50	4.48	Aut.'83	Sum.'86	23.5	−0.06	1.25	1.25	1.35	14.5
					Win.'86	8.5	−0.04	0.75	0.63	0.70	18
					Sum.'87	25.0	−0.05	1.52	1.52	1.63	18
San Fernando	8	3.97	3.92	Sum.'83	Sum.'86	25.0	−0.04	1.20	1.28	1.57	19
					Aut.'86	9.0	0.00	0.08	0.45	0.27	20
					Sum.'87	22.5	−0.05	1.70	1.86	2.00	20
San Rafael	9	4.23	3.77	Aut.'83	Sum.'86	25.5	−0.06	1.05	0.95	0.85	18
					Aut.'86	12.5	0.00	0.25	0.30	0.25	24
					Sum.'87	23.0	−0.05	1.62	1.60	1.55	20
Cocharcas	10	4.56	4.52	Aut.'82	Win.'86	11.7	−0.03	0.35	0.65	0.40	20
Concepción	11	3.42	3.39	Win.'84	Win.'86	13.0	−0.01	0.20	0.20	0.11	16
					Sum.'87	23.5	−0.04	0.44	0.44	1.12	18
Cabrero	12	3.50	3.52	Aut.'84	Win.'86	11.0	−0.02	0.27	0.50	0.50	20
					Sum.'87	28.0	−0.04	0.68	0.70	0.76	20
Laja	13	4.52	4.62	Win.'82	Win.'86	9.3	−0.02	0.18	0.36	0.25	20
					Sum.'87	26.0	−0.06	1.12	1.22	1.12	16
C. Esperanza	14	4.42	4.70	Aut.'79	Win.'86	10.0	−0.01	0.10	0.58	0.49	21
					Sum.'87	26.5	−0.06	1.44	1.57	1.82	14
Victoria	15	4.00	4.02	Aut.'84	Win.'86	9.5	−0.01	0.12	0.12	0.12	24
					Sum.'87	23.0	−0.03	0.52	0.50	0.56	16
Temuco	16	4.55	4.47	Aut.'81	Win.'86	11.5	0.00	0.06	0.13	0.07	20
					Sum.'87	23.0	−0.03	0.61	0.66	0.38	16
Gorbea	17	4.47	4.49	Aut.'83	Win.'86	9.0	−0.02	0.38	0.40	0.34	24
					Sum.'87	23.0	−0.04	0.62	0.62	0.72	16
Loncoche	18	4.03	3.84	Spr.'84	Win.'86	4.5	−0.02	0.30	0.22	0.20	20
					Sum.'87	17.2	−0.05	0.53	0.49	0.68	15
Mariquina	19	4.55	4.44	Aut.'83	Win.'86	2.8	−0.03	0.50	0.42	0.40	20
					Sum.'87	23.0	−0.04	0.96	0.96		15
Mafil	20	4.48	4.55	Spr.'83	Win.'86	5.1	−0.02	0.15	0.25	0.17	19
					Sum.'87	23.1	−0.04	1.30	1.38	1.29	16
Rio Bueno	21	4.50	4.48	Sum.'83	Win.'86	3.2	−0.04	0.19	0.19	0.25	16
					Sum.'87	24.0	−0.03	0.80	1.21	1.09	14

*Winter data are relative to the day minimum and do not represent the total corner uplift

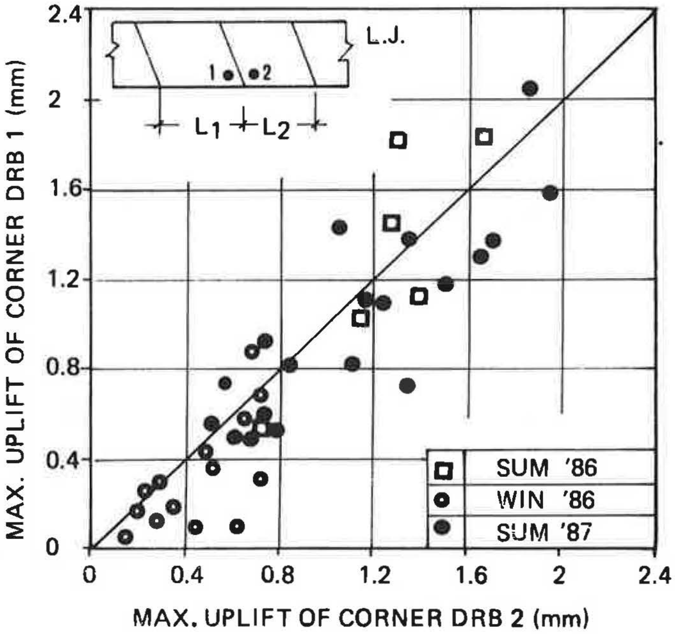

FIGURE 12 Comparison between maximum uplifts of adjoining corners (data from 21 test sections).

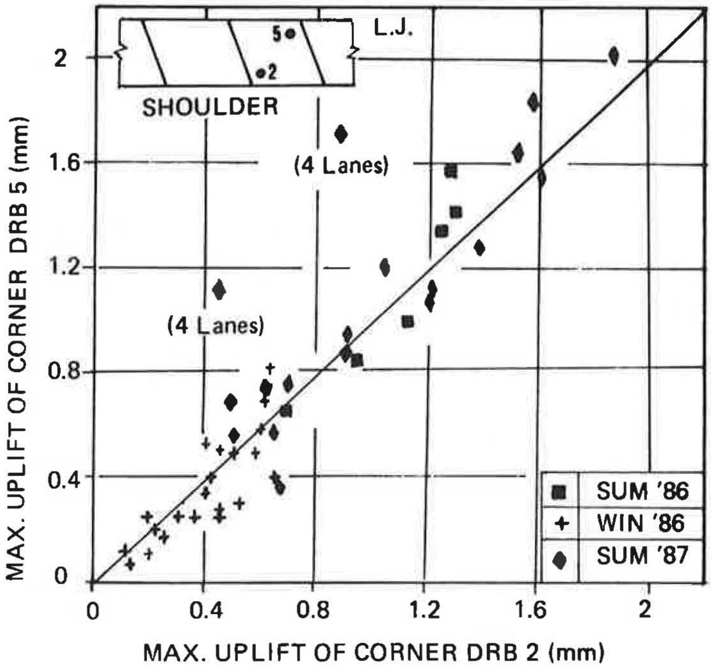

FIGURE 13 Comparison between maximum uplifts of opposite corners (data from 21 test sections).

pronounced opening of the joints, appear to be the prevailing unfavorable boundary conditions of the pavement slabs, which differs from the full support assumption usually considered in the engineering design of concrete pavements (*11, 12*). Conversely, the situation represented by the downward "cylindrical" shape is considered comparatively less detrimental.

These findings satisfactorily explain the distress that is being observed in some newer pavements where there are no signs of pumping, and whose cracking usually develops transversely at the middle of the slab, starting from the longitudinal edge. In addition, it has been verified through boreholes at the test section slabs that cracks start from the surface and move downward.

Detailed evaluation of the internal stresses with the superimposed nonlinear effects of environmental and wheel loads, calibrated with these results, is under way.

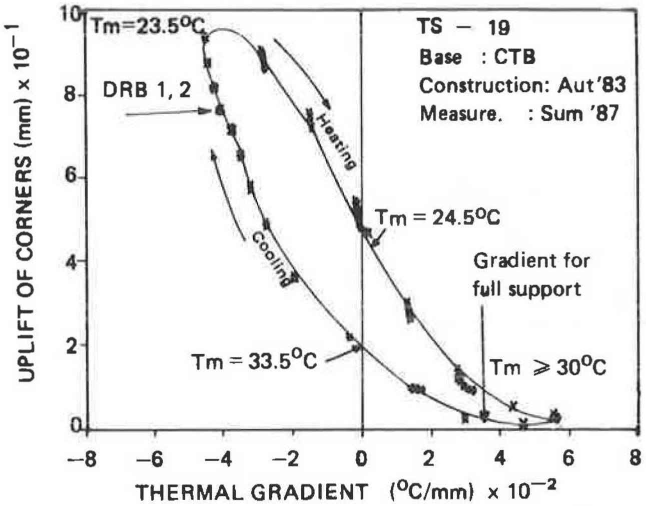

FIGURE 14 Slab corner displacements due to thermal gradient changes for new pavement in south region.

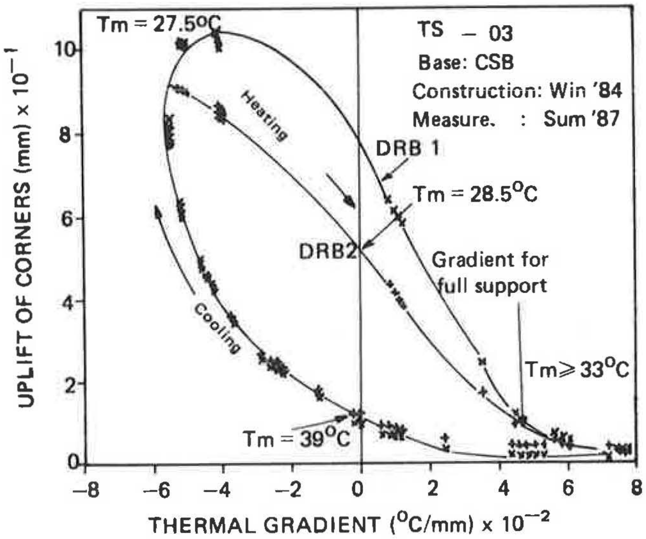

FIGURE 15 Slab corner displacements due to thermal gradient changes for new pavement in central region.

ACKNOWLEDGMENTS

The authors thank the Highway Division of the Ministry of Public Works for its permission to publish the results presented here. Special acknowledgments are given to the Concrete Pavement Group at the Institute of Research and Testing of Materials, IDIEM, for their constant assistance and support.

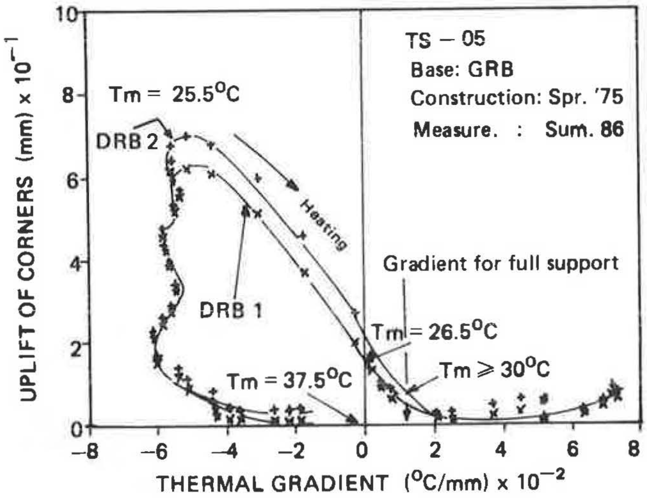

FIGURE 16 Slab corner displacements due to thermal gradient changes for old pavement in central region.

REFERENCES

1. Chilean Ministry of Public Works. Highway Maintenance and Rehabilitation Program in Chile. Presented at 2nd North American Conference on Managing Pavements, Toronto, Canada, 1987.
2. L. Ortega and P. Spratz. Performance Measures on Plain Concrete Pavements Without Dowels. *Proc., International Conference on Roads and Developments,* Paris, 1984, pp. 199–204.
3. A. Garcia. *Study of Rainfall Infiltration in a Concrete Pavement Structure,* Master's thesis, University of Chile, 1986 (in Spanish).
4. F. N. Hveem. Slab Warping Affects Pavement Performance. *Proc. ACI,* Vol. 47, 1951, pp. 797–808.
5. B. Tremper and D. L. Spellman. Shrinkage of Concrete—Comparison of Laboratory and Field Performance. In *Highway Research Record 3,* HRB, National Research Council, Washington, D.C., 1963, pp. 30–61.
6. IDIEM, University of Chile. *Field Instrumentation, Equipment and Measurement Methodology.* Highway Division, Chilean Ministry of Public Works. 1986 (in Spanish).
7. P. Ceza. *Study of the Temperature Distribution in a Concrete Pavement Structure.* Master's thesis, University of Chile, 1986 (in Spanish).
8. A. Neville. *Properties of Concrete.* Pitman Publishing Ltd., 1975.
9. "Curing Concrete" and "Volume Changes of Concrete." In *Design and Control of Concrete Mixtures.* PCA, 1984.
10. IDIEM, University of Chile. Concrete Pavements Research Project. *Annual Report 1986,* Vol. II. Highway Division, Chilean Ministry of Public Works. (in Spanish).
11. R. Packard. *Thickness Design for Concrete Highway and Street Pavements.* Portland Cement Association, 1984.
12. *AASHTO Interim Guide for Design of Pavement Structures, 1972.* American Association of State Highway and Transportation Officials, Chapter III, rev. 1981, pp. 25–36.

Publication of this paper sponsored by Committee on Rigid Pavement Design.